HOW DOES THE PRE-TRAINED FACE FAMILIARITY AFFECT THE DECODABILITY OF IDENTITY-SPECIFIC EEG REPRESENTATIONS?

Anonymous authors
Paper under double-blind review

ABSTRACT

While EEG-based visual decoding has attracted enormous interests and illustrated strong potentials over recent years, fine-grained facial identity decoding directly from brain-perceived EEGs has proved to be extremely difficult and challenging. In this paper, we investigate whether a pre-trained face familiarity can improve the discriminability and decodability of identity-related EEG representations. To address the challenge of identity decoding with fine-grained representations and sharing of highly similar visual features, we propose an EEG Spatio-Temporal Adaptive Fourier Fusion Network (EEG-STAFF) to effectively model complementary spatiotemporal and spectral information, which is supported by our establishment of a controlled and pre-trained familiarization paradigm for facial identity decoding. Experiments consistently show the improved identity decoding performances with the pre-trained familiarization, where the strongest gains emerge at the duration of 100-300ms, whist representation analysis reveals greater within-identity compactness and inter-identity separation. Compared with the existing representational state of the arts in relevant areas, the proposed EEG-STAFF achieves the best overall decoding performances, suggesting that the pre-trained face familiarization enhances the identity related neural representations and improves the EEG-based identity decoding.

1 INTRODUCTION

EEG-based visual decoding has made substantial progress, from object-category classification to large-scale visual representation learning (Spampinato et al., 2017; Grootswagers et al., 2022; Song et al., 2024). More recently, EEG-Face (Zhang et al., 2025) extended this direction to 40-way EEG-based face-identity decoding, demonstrating its feasible potential while also revealing its challenges. Unlike conventional object recognition, identity decoding requires fine-grained discrimination within a single semantic category, where identities share substantial structural features and differ only in subtle identity-specific cues. Human face recognition, on the other hand, is strongly influenced by familiarity. In other words, humans recognize familiar individuals reliably across changes in poses, illuminations, expressions, and appearances, whereas unfamiliar-face recognition is considerably more difficult (Popova & Wiese, 2023b). Neural studies similarly show that familiarity modulates face-evoked EEG responses (Wiese et al., 2019; Ambrus et al., 2021; Li et al., 2022), and recent evidences suggest that identity-related neural representations themselves can vary with familiarity (Kovács et al., 2023; Yan et al., 2023). This raises a natural question for EEG decoding: would such familiarity be exploited further to either introduce an additional familiarity-related response, or even make the identity information embedded inside EEG sequences more discriminative and easier to decode?

Existing studies have primarily examined familiarity through event-related potential (ERP) components, frequency-tagged responses, or relatively small-scale multivariate analyses of identity-related neural activities. While these studies have revealed when and how familiarity modulates neural responses, little attention has been paid to whether such changes translate into improved EEG identity decoding, or how such familiarity affects the temporal dynamics and learned representations underlying the decoding performances. As a result, the impact of familiarization on large-scale multi-class EEG-based identity decoding remains largely unexplored.

Reviewers: please read the Reviewer Guidelines (iclr.cc/Conferences/2027/ReviewerGuidelines) and the AI Policy for Reviewers (iclr.cc/Conferences/2027/AIPolicyForReviewers). If you used AI to expand, edit, or polish your review, please provide the input text to the LLM. Better still, consider skipping the LLM and submitting your original text: we, and the authors, are much more interested in your unedited thoughts than in what an LLM has to say. AI-assisted or not, you are putting your name and reputation behind your review: LLM-generated falsehoods, hallucinations or misrepresentations are subject to disciplinary action, which may include desk-rejecting all papers you have authored.

To address this question, we construct a pre-trained familiarization paradigm involving 40 initially unfamiliar identities. Specifically, participants first complete a Pre-Familiarization (Pre-Fam) EEG recording session, then learn the same identities through a dedicated "Face–Name" familiarization procedure using a separate face image set, and finally complete a Post-Familiarization (Post-Fam) EEG session. We evaluate familiarity-associated changes from multiple perspectives, including decoding performances, temporal dynamics, occipito-temporal ERP responses, and learned representation geometries.

Across five participants and multiple EEG decoding architectures, Post-Fam consistently yields higher identity-decoding performance than Pre-Fam. The improvement is temporally non-uniform, with the strongest gains concentrated between approximately 100 and 300 ms after stimulus onset. ERP analysis reveals condition differences over similar occipito-temporal intervals, while feature-space analysis shows greater within-identity compactness and inter-identity separation after the pre-trained familiarization. To exploit such pre-trained familiarization and thus characterize the obtained effectiveness more sensitively, we further propose an EEG Spatio-Temporal Adaptive Fourier Fusion Network (EEG-STAFF) to integrate complementary spatiotemporal and frequency-domain representations for EEG identity decoding.

Our main contributions are:

- We introduce a controlled pre-trained familiarization paradigm for 40-way EEG-based identity decoding and systematically examine how such acquired familiarity relates to the identity decodability.
- We characterize the familiarity-associated effectiveness across decoding architectures, temporal windows, occipito-temporal ERP responses, and learned representation geometries, revealing a consistent Post-Fam advantage that is most pronounced during the 100–300 ms interval.
- We propose EEG-STAFF, a dual-branch EEG decoder that jointly models spatiotemporal and frequency-domain information, achieving improved multi-class identity performances in comparison with the existing representative EEG baselines.

2 Related Work

2.1 EEG-based Visual Decoding

EEG-based visual decoding has recently attracted increasing attention and has progressed from category-level classification toward large-scale visual representation learning. Early work demonstrated that EEG responses elicited by natural images contain discriminative information about visual object categories (Spampinato et al., 2017; Palazzo et al., 2020). More recent large-scale datasets, including THINGS-EEG (Grootswagers et al., 2022) and related high-trial visual EEG benchmarks (Gifford et al., 2022), have enabled the study of neural representations over natural images and object concepts. Building on these datasets, contrastive and multimodal approaches such as NICE-EEG (Song et al., 2024) align EEG responses with pretrained visual representations, extending EEG decoding to large-scale and zero-shot object recognition. EEG signals have also been explored for image-level classification and reconstruction (Guenther et al., 2024).

These studies have substantially advanced EEG representational learning, but they mainly focus on coarse-grained semantic categories, where different classes have large visual and semantic differences. In contrast, identity-level decoding is more challenging since all stimuli belong to the same semantic category and differ only in subtle identity-specific facial cues. EEG-Face (Zhang et al., 2025) extends EEG visual decoding to this task by examining 40-way face-identity recognition from image-evoked EEGs, demonstrating the feasible potential of identity-level decoding while also revealing the difficulty of differentiating highly similar facial identities. Instead of treating this challenge primarily as a modeling problem, our approach is to focus on improving the effectiveness of EEG representations by introducing the pre-trained familiarity to increase its identity discriminative capability at the source.

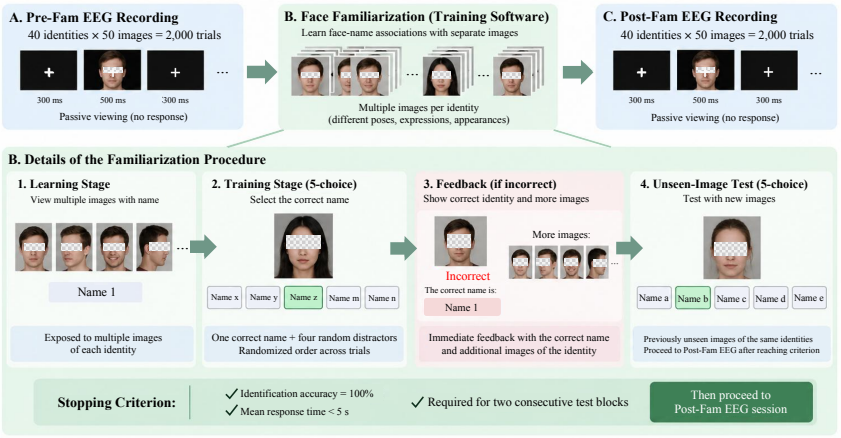


Figure 1: Overview of the experimental paradigm and face familiarization procedure, where participants completed Pre-Fam and Post-Fam EEG sessions upon 40 identities across 2,000 EEG stimulus images, and familiarization was performed between the two sessions using a separate image set.

2.2 Face Familiarity and Identity Representation

ERP studies have reported familiarity-sensitive activities emerging from approximately 200 ms and becoming more pronounced at later processing stages (Caharel et al., 2014; Wiese et al., 2019; Ambrus et al., 2019). Importantly, these effects depend on how familiarity is acquired (Collins et al., 2018; Dalski et al., 2022; Wiese et al., 2024a). Following real-life personal familiarization, Ambrus et al. (2021) observed the strongest familiarity-related representations, with weaker effects after media-based familiarization and no robust effects after brief perceptual exposure, suggesting that the quality of familiarization plays an important role beyond repeated visual exposure alone. Beyond conventional ERP contrasts, multivariate EEG analyses have further shown that familiarity itself can be decoded from neural activities, with prominent familiarity-related information emerging during later post-stimulus periods (Li et al., 2022). More recent studies have examined how familiarity interacts with identity processing. Kovács et al. (2023) showed that identity information emerges at approximately 100 ms, while its discriminability at later stages varies with familiarity. Frequency-tagging studies similarly reported stronger image-generalizable identity-specific responses for familiar than unfamiliar faces (Yan et al., 2020; 2023). Longitudinal evidences further suggests that identity-specific neural responses can increase when initially unfamiliar individuals become familiar through real-world interaction (Campbell & Tanaka, 2021; Popova & Wiese, 2023a; Wiese et al., 2024b).

Despite these findings, prior work has predominantly approached familiarity from a cognitive-neuroscience perspective, focusing on ERP components, frequency-tagged responses, or multivariate characterization of familiarity- and identity-related neural activities. Comparatively less known is how the experimentally acquired familiarity affects the performance and representation structure of large-scale multi-class EEG identity decoding. In particular, whether familiarization systematically improves the discriminability of facial identities under a fixed identity space remains underexplored. Our work addresses this gap by directly examining how controlled familiarization affects 40-way EEG identity decoding, including its temporal dynamics, and the geometry of learned identity representations.

3 Experimental Protocol

Fig. 1 illustrates our proposed pre–post familiarization paradigm, consisting of a Pre-Fam EEG recording session, an intervening face-familiarization stage, and a Post-Fam EEG recording session. The two EEG recording sessions use the same identities and stimulus images, while familiarization is performed using a separate image set of the same identities.

3.1 PARTICIPANTS, STIMULI, AND EEG ACQUISITION

Participants and EEG viewing task. EEG data were collected from five healthy right-handed male participants (age: 23.2 ± 2.9 years), all of whom had normal or corrected-to-normal vision and reported no history of neurological disorders. Each participant completed two EEG recording sessions with the same 40 identities: a Pre-Fam session before familiarization, when all identities were initially unfamiliar, and a Post-Fam session after familiarization. As illustrated in Fig. 1(A) and Fig. 1(C), each trial consisted of a 300 ms fixation period followed by a 500 ms face presentation. Participants passively viewed the faces without making any behavioral response and were instructed to minimize unnecessary movements.

Stimuli. The EEG stimulus set comprised 40 identities with 50 visually diverse images per identity, yielding 2,000 face images in total. Images of the same identity varied in appearance while sharing the same identity label, reducing reliance on image-specific low-level cues. The same 2,000 images were presented in both EEG sessions to keep the visual input consistent across Pre and Post Fam.

EEG acquisition. EEG was recorded using a 128-channel GREENTEK system at 5,000 Hz and downsampled to 1,000 Hz. After preprocessing, each trial yielded a 126×500 EEG matrix over 0–500 ms; full preprocessing details are provided in Appendix. A.5.

3.2 FACE FAMILIARIZATION

As shown in Fig. 1(B), the familiarization procedure comprised three stages: learning, recognition training, and unseen-image evaluation. During the learning stage, participants repeatedly viewed multiple images of each identity together with the corresponding name. They then completed a face recognition task with five-alternative forced-choice (5-AFC) by using the same familiarization images, where each face was paired with one correct name and four randomly sampled distractors. Candidate positions were randomized, and incorrect responses were followed by feedback indicating the correct identity.

After training, participants completed a 5-AFC evaluation via using previously unseen images of the same identities to assess whether their recognition could generalize beyond the images used during learning and training. Participants would not proceed to the Post-Fam EEG session until they achieved 100% recognition rate with a mean response time ≤ 5 s in two consecutive evaluation blocks.

To reduce image-specific memorization during familiarization, we use a separate image set that is not presented in either EEG session. Meanwhile, identical EEG stimuli are used in the Pre-Fam and Post-Fam sessions to control the visual input across conditions.

4 METHOD

Fig. 2 illustrates an architectural overview of our proposed network EEG-STAFF. As seen, EEG-STAFF is a dual-branch network that learns complementary spatiotemporal and spectral representations for EEG-based identity decoding. While the spatiotemporal branch captures identity-relevant electrode–temporal patterns, the spectral branch models global frequency-domain information. The two representations are adaptively fused using trial-specific weights and fed into a classifier for identity prediction.

4.1 CHANNEL-SPATIOTEMPORAL ATTENTION MODULE

Following shallow feature extractions, the EEG representation is refined by a Channel-Spatiotemporal Attention Module (CSAM), adapted from Convolutional Block Attention Module (CBAM) (Woo et al., 2018). CSAM sequentially applies two attention units, including channel attention and spatiotemporal attention. While channel attention reweights learned feature channels using global average and max pooling with a shared MLP, spatiotemporal attention further emphasizes informative responses across electrodes and temporal dimensions through pooled feature maps and convolutional attentions.

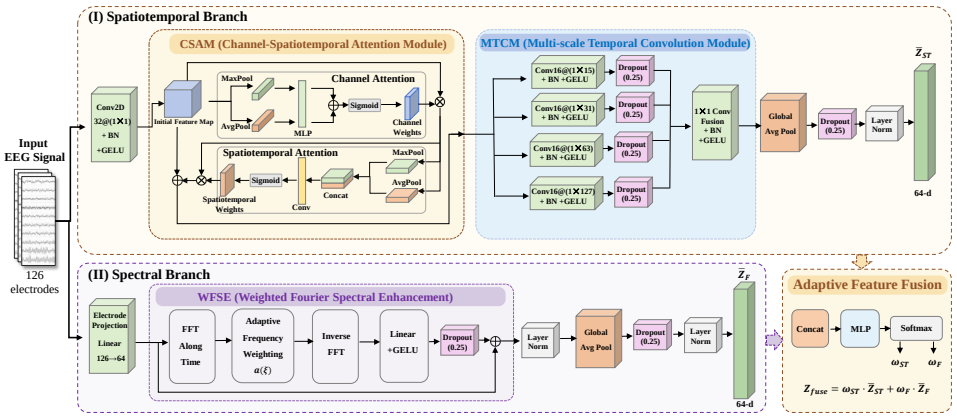


Figure 2: Overview of EEG-STAFF, comprising a CSAM–MTCM spatiotemporal branch, a spectral branch, and adaptive feature fusion for identity decoding. $\otimes$ and $\oplus$ denote element-wise multiplication and addition, respectively.

The two attention units are applied sequentially with residual enhancement, which can be described as:

$$\mathbf{F}_{\mathrm{CSAM}} = \mathbf{F}_0 + \mathbf{M}_{\mathrm{Sp}}\left(\mathbf{M}_{\mathrm{C}}(\mathbf{F}_0) \odot \mathbf{F}_0\right) \odot \left(\mathbf{M}_{\mathrm{C}}(\mathbf{F}_0) \odot \mathbf{F}_0\right), \tag{1}$$

where $\mathbf{F}_0$ denotes the shallow EEG feature map, $\mathbf{M}_{\mathrm{C}}$ and $\mathbf{M}_{\mathrm{Sp}}$ denote the channel-attention and spatiotemporal attention maps, respectively, and $\odot$ denotes element-wise multiplication. The residual connection preserves the original EEG representation while enhancing identity-discriminative responses. The resulting features are subsequently refined and pooled to obtain the spatiotemporal representation $\mathbf{Z}_{\mathrm{ST}}$.

4.2 Multi-scale Temporal Convolution Module

To better explore the temporal features of EEG data for identity decoding, we employed the idea of Inception modules (Szegedy et al., 2015) to construct a Multi-scale Temporal Convolution Module (MTCM). This module aims to extract EEG features at four temporal scales, and the corresponding convolutional kernels are 1×127, 1×63, 1×31, and 1×15, respectively. After the multi-scale convolution layer, a 1×1 convolution is further used to fuse the multi-scale features. Finally, global average pooling is applied to aggregate the temporal features and reduce the feature dimensionality.

4.3 Weighted Fourier Spectral Enhancement Module

While the spatiotemporal branch models localized activities across electrodes and time, the spectral branch captures complementary frequency-domain information using Weighted Fourier Spectral Enhancement (WFSE). Specifically, the 126-channel EEG signal is first projected into a 64-dimensional feature sequence by a bias-free linear transformation, while preserving the temporal resolution. WFSE then applies a Fourier transform along the temporal dimension.

Unlike conventional Fourier Neural Operators that operate on a predefined subset of Fourier modes Li et al. (2020), WFSE retains all modes within the preserved EEG bandwidth and learns their relative importance. For each frequency mode ξ_k, we define

$$a(\xi_k) = 2\sigma(g_k), \tag{2}$$

where g_k is a learnable scalar and $\sigma(\cdot)$ denotes the sigmoid function. We initialize $g_k = 0$ as such that $a(\xi_k) = 1$ at the beginning of training. The frequency-enhanced representation is computed as

$$\mathcal{K}(\mathbf{V}) = \mathcal{F}^{-1}\left[a(\boldsymbol{\xi}) \odot \mathcal{F}(\mathbf{V})\right]. \tag{3}$$

In comparison with the existing work, our proposed WFSE avoids hard frequency truncation while allowing the network to suppress less informative components and emphasize identity-relevant spectral patterns. The resulting features are further refined by a point-wise linear transformation, nonlinear activation, residual connection, and normalization, yielding a frequency-enhanced representation for subsequent feature fusion and identity decoding.

4.4 Adaptive Feature Fusion

For the same EEG trial, the spatiotemporal and spectral branches produce complementary representations $\mathbf{Z}_{\mathrm{ST}}$ and $\mathbf{Z}_{\mathrm{F}}$, respectively. To adaptively balance their contributions, we normalize and concatenate the two branch features and use a lightweight MLP to predict trial-specific fusion weights, details of which can be described below:

$$[\omega_{\mathrm{ST}}, \omega_{\mathrm{F}}] = \mathrm{Softmax}\left(\mathrm{MLP}\left([\bar{\mathbf{Z}}_{\mathrm{ST}}; \bar{\mathbf{Z}}_{\mathrm{F}}]\right)\right), \tag{4}$$

where $\omega_{\mathrm{ST}} + \omega_{\mathrm{F}} = 1$. The fused representation is

$$\mathbf{Z}_{\mathrm{fuse}} = \omega_{\mathrm{ST}} \bar{\mathbf{Z}}_{\mathrm{ST}} + \omega_{\mathrm{F}} \bar{\mathbf{Z}}_{\mathrm{F}}. \tag{5}$$

This trial-adaptive fusion dynamically balances spatiotemporal and spectral information. The fused representation is fed into a linear classifier, and the entire network is trained end-to-end using cross-entropy loss.

5 Experiments

5.1 Experimental Setup

We evaluate EEG-based face-identity decoding under the Pre-Fam and Post-Fam conditions. Unless otherwise specified, all models use the full post-stimulus interval from 0 to 500 ms as input.

Evaluation protocol. Experiments are conducted independently for each participant using five-fold cross-validation. For each identity, the 50 trials corresponding to 50 distinct face images are partitioned into five non-overlapping folds of 10 trials. In each fold, 40 trials per identity are used for training and 10 for testing, yielding 1,600 training trials and 400 test trials. Each image is used for testing exactly once across the five folds. To ensure a controlled Pre-Fam and Post-Fam comparison, we use identical image-level splits in both conditions. Thus, each fold contains the same training and test face images before and after familiarization, and only the corresponding EEG responses differ across the two recording sessions.

Comparison methods. We compare EEG-STAFF with four representative EEG decoders: EEGNet (Lawhern et al., 2018), SyncNet (Li et al., 2017), EEGConformer (Song et al., 2023), and DAEEGViT (Ouyang et al., 2025), covering compact convolutional, synchronization-based, and attention-based modeling paradigms. All methods use the same preprocessed inputs, data splits, and evaluation protocol for fair comparisons. All models are implemented in PyTorch and trained with AdamW using an initial learning rate of 1×10^{-3}, a batch size of 64, and 200 epochs unless otherwise specified. Experiments are conducted on a single NVIDIA A100-PCIE-40GB GPU.

5.2 Analysis of Identity Decoding Results Improved by Familiarization

Table 1 reports participant-wise Top-1 and Top-5 accuracy rates under Pre-Fam and Post-Fam conditions. A consistent Post-Fam advantage is observed across all five participants and all the five compared decoders. This consistency suggests that the observed improvement reflects a systematic change in identity-related EEG representations rather than an effect specific to a particular decoder.

Table 2 summarizes the results averaged across participants. All methods show positive gains after familiarization, with Top-1 improvements ranging from $+1.79\%$ to $+2.70\%$ and Top-5 improvements ranging from $+3.13\%$ to $+6.16\%$. The effect is therefore evident not only in the most likely identity prediction, but also in the broader rank structure captured by Top-5 accuracy rates. Across methods, it can also be seen that the performance of Post-Fam consistently exceeds the corresponding Pre-Fam, providing a converging validation that pre-trained familiarity is associated with more decodable identity information in EEG responses. Among the evaluated decoders, EEG-STAFF achieves the highest decoding performance in both conditions and the largest overall Pre-Fam-to-Post-Fam gain.

While the best Top-1 rate achieved by EEG-STAFF at 7.81% is far away from the normal face recognition rates achieved in the community of computer vision, we argue it is still encouraging and

Table 1: Listing of identity decoding results before and after familiarization across five participants, which are reported as mean ± SD over three random seeds.

Method	Condition	Subj 1		Subj 2		Subj 3		Subj 4		Subj 5	
		Top-1	Top-5	Top-1	Top-5	Top-1	Top-5	Top-1	Top-5	Top-1	Top-5
EEGNet	Pre-Fam	$3.97_{\pm 0.42}$	$17.28_{\pm 1.12}$	$3.57_{\pm 0.47}$	$16.67_{\pm 1.20}$	$4.01_{\pm 0.39}$	$17.24_{\pm 1.08}$	$4.30_{\pm 0.44}$	$17.58_{\pm 1.16}$	$3.64_{\pm 0.50}$	$16.32_{\pm 1.25}$
	Post-Fam	$4.98_{\pm 0.40}$	$19.38_{\pm 1.10}$	$5.43_{\pm 0.44}$	$20.02_{\pm 1.16}$	$6.21_{\pm 0.38}$	$22.46_{\pm 1.05}$	$6.41_{\pm 0.41}$	$23.24_{\pm 1.08}$	$5.97_{\pm 0.46}$	$21.20_{\pm 1.20}$
SyncNet	Pre-Fam	$3.85_{\pm 0.45}$	$16.98_{\pm 1.18}$	$3.53_{\pm 0.51}$	$16.61_{\pm 1.26}$	$3.91_{\pm 0.43}$	$17.54_{\pm 1.14}$	$4.56_{\pm 0.48}$	$17.69_{\pm 1.21}$	$3.74_{\pm 0.46}$	$16.42_{\pm 1.30}$
	Post-Fam	$5.36_{\pm 0.43}$	$20.00_{\pm 1.14}$	$5.00_{\pm 0.48}$	$18.69_{\pm 1.22}$	$5.90_{\pm 0.40}$	$21.35_{\pm 1.09}$	$6.28_{\pm 0.45}$	$21.50_{\pm 1.15}$	$6.00_{\pm 0.42}$	$19.35_{\pm 1.18}$
EEGConformer	Pre-Fam	$4.55_{\pm 0.31}$	$17.57_{\pm 0.95}$	$4.58_{\pm 0.34}$	$17.54_{\pm 1.02}$	$4.81_{\pm 0.28}$	$18.50_{\pm 0.90}$	$5.09_{\pm 0.30}$	$18.99_{\pm 0.93}$	$4.82_{\pm 0.33}$	$17.69_{\pm 0.98}$
	Post-Fam	$7.03_{\pm 0.29}$	$23.03_{\pm 0.91}$	$7.13_{\pm 0.31}$	$23.06_{\pm 0.95}$	$7.44_{\pm 0.27}$	$24.38_{\pm 0.86}$	$7.43_{\pm 0.28}$	$24.33_{\pm 0.88}$	$7.28_{\pm 0.30}$	$23.06_{\pm 0.92}$
DAEEGViT	Pre-Fam	$4.69_{\pm 0.29}$	$17.76_{\pm 0.90}$	$4.55_{\pm 0.32}$	$17.51_{\pm 0.96}$	$4.72_{\pm 0.27}$	$18.14_{\pm 0.88}$	$5.06_{\pm 0.28}$	$18.87_{\pm 0.91}$	$4.86_{\pm 0.30}$	$17.80_{\pm 0.94}$
	Post-Fam	$7.21_{\pm 0.27}$	$23.34_{\pm 0.87}$	$7.15_{\pm 0.30}$	$23.15_{\pm 0.90}$	$7.40_{\pm 0.25}$	$24.16_{\pm 0.83}$	$7.57_{\pm 0.26}$	$24.44_{\pm 0.85}$	$7.35_{\pm 0.28}$	$23.29_{\pm 0.88}$
EEG-STAFF	Pre-Fam	$\mathbf{5.22}_{\pm 0.24}$	$\mathbf{19.56}_{\pm 0.82}$	$\mathbf{5.00}_{\pm 0.27}$	$\mathbf{18.16}_{\pm 0.88}$	$\mathbf{5.02}_{\pm 0.25}$	$\mathbf{18.69}_{\pm 0.84}$	$\mathbf{5.30}_{\pm 0.23}$	$\mathbf{19.53}_{\pm 0.80}$	$\mathbf{5.03}_{\pm 0.26}$	$\mathbf{17.08}_{\pm 0.86}$
	Post-Fam	$\mathbf{7.88}_{\pm 0.22}$	$\mathbf{25.61}_{\pm 0.79}$	$\mathbf{7.76}_{\pm 0.24}$	$\mathbf{23.87}_{\pm 0.84}$	$\mathbf{7.78}_{\pm 0.23}$	$\mathbf{24.87}_{\pm 0.81}$	$\mathbf{8.02}_{\pm 0.21}$	$\mathbf{26.75}_{\pm 0.77}$	$\mathbf{7.60}_{\pm 0.25}$	$\mathbf{22.70}_{\pm 0.86}$

Table 2: Average identity decoding improvement after familiarization. Results are averaged across five participants. Gain denotes the Post-Fam improvement over Pre-Fam/Post-Fam in percentage.

Method	Top-1 Accuracy (%)			Top-5 Accuracy (%)		
	Pre	Post	Gain	Pre	Post	Gain
EEGNet	3.90	5.80	+1.90	17.02	21.26	+4.24
SyncNet	3.92	5.71	+1.79	17.05	20.18	+3.13
EEGConformer	4.77	7.26	+2.49	18.06	23.57	+5.51
DAEEGViT	4.78	7.34	+2.56	18.02	23.68	+5.66
EEG-STAFF	**5.11**	**7.81**	**+2.70**	**18.60**	**24.76**	**+6.16**

sufficient to validate the effectiveness of our proposed network model and the familiarity paradigm introduced, considering the fact that: (i) the best Top-1 accuracy achieved by EEG-Face (Zhang et al., 2025) is 3.4%, marginally above the chance level; and (ii) the best Top-1 rate for general object classification/decoding is only reported at 7% (Ahmed et al., 2021), which is known to be less challenging compared with the fine-grained identity decoding.

5.3 Temporal Dynamics of Familiarity-Enhanced Identity Decoding

Having established that identity decoding is improved with the pre-trained familiarization, we next investigate when this advantage emerges across the brain responding period, i.e. 0-500ms. We divide the period of 0–500 ms into five consecutive 100-ms windows and perform identity decoding independently within each window using the same participant-wise data partitions as that of the full window analysis. This analysis of temporal dynamics allows us to determine whether the familiarity-associated gain is distributed uniformly over time or not.

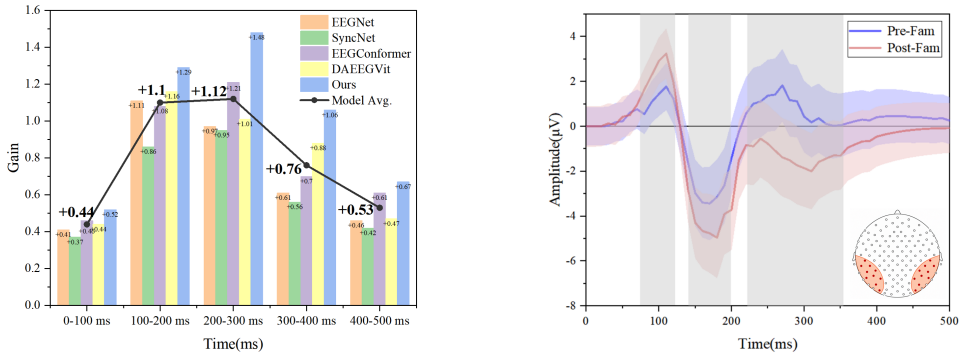
Table 3 reports the Top-1 decoding accuracy rate within each temporal window. Across all five models compared, Post-Fam consistently outperforms Pre-Fam in every window, indicating that the familiarity-associated improvement is not restricted to a specific model or time interval. As shown in Fig. 3(a), however, the gain is clearly concentrated in the intermediate post-stimulus period. Specifically, the model-averaged gain is only $+0.44$ during 0–100 ms, but increases to $+1.10$ and $+1.12$ during 100–200 and 200–300 ms, respectively, although positive gains still remain evident at later intervals, reaching $+0.76$ during 300–400 ms and $+0.53$ during 400–500 ms.

This concentration within 100–300 ms is consistent across all compared models. EEGNet and DAEEGViT show their largest gains during 100–200 ms, whereas SyncNet, EEGConformer, and EEG-STAFF peak during 200–300 ms. Notably, EEG-STAFF exhibits the largest improvement in every temporal window, reaching $+1.48$ during 200–300 ms. In summary, these results show that familiarization enhances identity decoding throughout the post-stimulus period, with the strongest and most consistent benefit emerging between 100 and 300 ms.

We further analyze event-related potentials (ERPs) over the bilateral occipito-temporal region, where face-sensitive responses such as the N170/N250 and later familiarity-related activity are commonly observed (Sun et al., 2026; Li et al., 2022; Eick et al., 2021). For a representative participant, we average signals from 10 occipito-temporal electrodes in each hemisphere to obtain a bilateral

Table 3: Listing of experimental results before and after familiarization, which are averaged across five participants and reported as mean ± SD of Top-1 accuracy (%).

Method	Condition	0–100 ms	100–200 ms	200–300 ms	300–400 ms	400–500 ms
EEGNet	Pre-Fam	$3.34_{\pm 0.28}$	$3.74_{\pm 0.34}$	$3.81_{\pm 0.37}$	$3.67_{\pm 0.33}$	$3.41_{\pm 0.29}$
	Post-Fam	$3.75_{\pm 0.31}$	$4.85_{\pm 0.41}$	$4.78_{\pm 0.44}$	$4.28_{\pm 0.39}$	$3.87_{\pm 0.35}$
SyncNet	Pre-Fam	$3.32_{\pm 0.27}$	$3.71_{\pm 0.33}$	$3.87_{\pm 0.36}$	$3.77_{\pm 0.35}$	$3.48_{\pm 0.30}$
	Post-Fam	$3.69_{\pm 0.30}$	$4.57_{\pm 0.38}$	$4.82_{\pm 0.46}$	$4.33_{\pm 0.42}$	$3.90_{\pm 0.34}$
EEGConformer	Pre-Fam	$4.49_{\pm 0.32}$	$4.61_{\pm 0.38}$	$4.72_{\pm 0.42}$	$4.71_{\pm 0.40}$	$4.68_{\pm 0.34}$
	Post-Fam	$4.95_{\pm 0.30}$	$5.69_{\pm 0.43}$	$5.93_{\pm 0.47}$	$5.41_{\pm 0.45}$	$5.29_{\pm 0.37}$
DAEEGViT	Pre-Fam	$4.41_{\pm 0.31}$	$4.47_{\pm 0.36}$	$4.59_{\pm 0.41}$	$4.67_{\pm 0.43}$	$4.66_{\pm 0.33}$
	Post-Fam	$4.85_{\pm 0.29}$	$5.63_{\pm 0.42}$	$5.60_{\pm 0.48}$	$5.55_{\pm 0.46}$	$5.13_{\pm 0.36}$
EEG-STAFF	Pre-Fam	$\mathbf{5.01}_{\pm 0.35}$	$\mathbf{5.07}_{\pm 0.39}$	$\mathbf{5.02}_{\pm 0.44}$	$\mathbf{5.06}_{\pm 0.38}$	$\mathbf{5.03}_{\pm 0.34}$
	Post-Fam	$\mathbf{5.53}_{\pm 0.33}$	$\mathbf{6.36}_{\pm 0.45}$	$\mathbf{6.50}_{\pm 0.49}$	$\mathbf{6.12}_{\pm 0.41}$	$\mathbf{5.70}_{\pm 0.36}$



(a) Decoding gains across the divided timing windows.

(b) Occipito-temporal ERP.

Figure 3: Identity decoding across temporal dynamics and ERP analysis of the pre-trained familiarity, including: (a) Top-1 decoding gains (Post-Fam minus Pre-Fam) across five windows for different EEG decoders; the black line denotes the average gain across models. (b) ERP responses over the bilateral occipito-temporal region for a representative participant. Colored bands denote SD, gray intervals indicate significant condition differences ($p < 0.05$), and the inset illustrates the bilateral occipito-temporal region of interest (ROI).

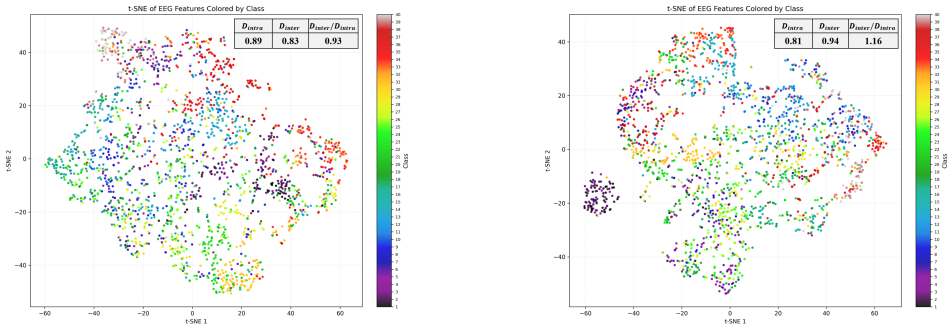
ERP waveform. As shown in Fig. 3(b), Pre-Fam and Post-Fam responses differ significantly across several post-stimulus intervals, where substantial overlap within the 100–300 ms range shows the strongest decoding gains. This is consistent with the familiarity-associated changes in occipito-temporal neural responses occurring within a similar time range as that of the observed decoding improvement.

5.4 Identity Representation Compactness and Separability

To examine whether the improved identity decoding with familiarization is reflected in the learned feature geometry. We extract penultimate-layer features of EEG-STAFF from held-out test trials and visualize them using t-SNE (Van der Maaten & Hinton, 2008) in Fig. 4. As seen, the Post-Fam representations exhibit more compact local identity structure and reduced overlap for several identities compared with Pre-Fam, although substantial overlap still remains, demonstrating again the extremely challenging nature of such a fine-grained identity decoding directly out of EEGs.

As t-SNE only provides a qualitative two-dimensional visualization, we additionally quantify the feature geometry in the original representation space using cosine-based intra- and inter-identity distances (D_{intra} and D_{inter}), computed on L_2-normalized features.Detailed definitions are provided in Appendix A.4.

The quantitative results embedded in Fig. 4 show that D_{intra} is reduced from 0.89 to 0.81, while D_{inter} increased from 0.83 to 0.94. Accordingly, the ratio $D_{\text{inter}}/D_{\text{intra}}$ is increased from 0.93 to 1.16. Together, the qualitative and quantitative results indicate that Post-Fam representations are



(a) Pre-Fam (b) Post-Fam

Figure 4: t-SNE visualization of EEG-STAFF identity representations under the Pre-Fam and Post-Fam conditions. Each point denotes one EEG trial, with colors indicating face identities.

Table 4: Ablation study of EEG-STAFF. Top-1 accuracy (%) is averaged across five participants.

Variant	Pre-Fam	Post-Fam	Gain
w/o WFSE	4.65	6.23	+1.58
w/o CSAM	4.21	5.67	+1.46
MTCM → Single-scale Conv.	4.43	5.83	+1.40
WFSE → Vanilla Fourier Transform	4.86	7.17	+2.31
Full EEG-STAFF	**5.11**	**7.81**	**+2.70**

more compact within identities and more separated across identities, consistent with the improved identity-decoding performance after the pre-trained familiarization.

Table 4 evaluates the contribution of the major components in EEG-STAFF. All ablated variants retain a positive Post-Fam gain, indicating that the familiarity-associated improvement is not induced by any single module. However, removing key components from either the spatiotemporal or spectral pathway degrades the performances. The spectral branch has a particularly strong effect. Removing WFSE causes a substantial performance drop, while replacing it with a Vanilla Fourier Transform recovers a large portion of the lost accuracy. This result highlights the importance of incorporating frequency-domain information into EEG identity decoding. The full WFSE further improves over the vanilla Fourier variant, showing that adaptive spectral reweighting provides additional benefit beyond simply transforming the signal into the frequency domain.

Similarly, removing CSAM or replacing multi-scale temporal modeling with a single-scale convolution reduces the decoding performance and weakens the familiarity-associated gain. Overall, these results show that EEG-STAFF benefits from both modeling localized spatiotemporal structure and global spectral information, where the spectral representation contributes more substantially to both identity decoding and the effectiveness of the pre-trained familiarization.

6 Conclusion

We investigated how acquired face familiarity relates to EEG-based identity decoding. Using a controlled pre–post familiarization paradigm, we consistently observed improved multi-class identity decoding after familiarization across participants and decoders. The improvement is temporally structured, with the strongest gains emerging between 100 and 300 ms, which is also supported by corresponding occipito-temporal ERP differences. Representational analysis further shows greater within-identity compactness and inter-identity separation after familiarization. We also developed EEG-STAFF to jointly model spatiotemporal and spectral EEG information, achieving improved identity decoding performances, forwarding the frontiers of the challenging problem of neural identity decoding further beyond chance levels (Zhang et al., 2025). Together, these findings suggest that face familiarity is associated not only with changes in neural responses, but also with more discriminative and decodable identity-related EEG representations, providing a new perspective on fine-grained EEG visual decoding.

AI USE STATEMENT

We confirm that generative AI tools are only used for English grammar checking and language polishing, and all AI assisted texts are carefully reviewed and verified for correctness by two authors. We also confirm that no generative AI tools are ever used for generating experimental results, conducting data analysis, or making scientific conclusions. We take full responsibility for the final content of this work, including all texts, claims, and artifacts produced with the assistance of generative AI.

ETHICS STATEMENT

This study involved human participants and was approved by the relevant institutional ethics committee. All participants provided written informed consent prior to participation, received monetary compensation, and were informed of their right to withdraw from the study at any time. EEG data were anonymized before analysis, and no personally identifiable information was used in the reported experiments.

REPRODUCIBILITY STATEMENT

We provide detailed descriptions of the experimental protocol, model architecture, training configuration, and evaluation procedure in Sections 3–5. Additional details on feature-geometry computation, EEG preprocessing, pre-experiment familiarity screening, behavioral validation, and occipito-temporal ROI definition are provided in Appendix A.4–A.7. The source code and implementation configurations required to reproduce the reported experiments are provided in the anonymous supplementary material.

REFERENCES

Hamad Ahmed, Ronnie B Wilbur, Hari M Bharadwaj, and Jeffrey Mark Siskind. Object classification from randomized eeg trials. In *2021 IEEE/CVF Conference on Computer Vision and Pattern Recognition (CVPR)*, pp. 3844–3853. IEEE, 2021.

Géza Gergely Ambrus, Daniel Kaiser, Radoslaw Martin Cichy, and Gyula Kovács. The neural dynamics of familiar face recognition. *Cerebral Cortex*, 29(11):4775–4784, 2019.

Géza Gergely Ambrus, Charlotta Marina Eick, Daniel Kaiser, and Gyula Kovács. Getting to know you: Emerging neural representations during face familiarization. *Journal of Neuroscience*, 41 (26):5687–5698, 2021.

Stephanie Caharel, Meike Ramon, and Bruno Rossion. Face familiarity decisions take 200 msec in the human brain: Electrophysiological evidence from a go/no-go speeded task. *Journal of Cognitive Neuroscience*, 26(1):81–95, 2014.

Alison Campbell and James W Tanaka. When a stranger becomes a friend: Measuring the neural correlates of real-world face familiarisation. *Visual Cognition*, 29(10):689–707, 2021.

Elliot Collins, Amanda K Robinson, and Marlene Behrmann. Distinct neural processes for the perception of familiar versus unfamiliar faces along the visual hierarchy revealed by eeg. *NeuroImage*, 181:120–131, 2018.

Alexia Dalski, Gyula Kovács, and Géza Gergely Ambrus. Evidence for a general neural signature of face familiarity. *Cerebral Cortex*, 32(12):2590–2601, 2022.

Charlotta M Eick, Géza G Ambrus, and Gyula Kovács. Inhibition of the occipital face area modulates the electrophysiological signals of face familiarity: A combined ctbs-eeg study. *Cortex*, 141: 156–167, 2021.

Alessandro T Gifford, Kshitij Dwivedi, Gemma Roig, and Radoslaw M Cichy. A large and rich eeg dataset for modeling human visual object recognition. *NeuroImage*, 264:119754, 2022.

Alex Graves. Long short-term memory. *Supervised sequence labelling with recurrent neural networks*, pp. 37–45, 2012.

Tijl Grootswagers, Ivy Zhou, Amanda K Robinson, Martin N Hebart, and Thomas A Carlson. Human eeg recordings for 1,854 concepts presented in rapid serial visual presentation streams. *Scientific Data*, 9(1):3, 2022.

Sven Guenther, Nataliya Kosmyna, and Pattie Maes. Image classification and reconstruction from low-density eeg. *Scientific Reports*, 14(1):16436, 2024.

Gyula Kovács, Chenglin Li, Géza Gergely Ambrus, and A Mike Burton. The neural dynamics of familiarity-dependent face identity representation. *Psychophysiology*, 60(9):e14304, 2023.

Vernon J Lawhern, Amelia J Solon, Nicholas R Waytowich, Stephen M Gordon, Chou P Hung, and Brent J Lance. Eegnet: a compact convolutional neural network for eeg-based brain–computer interfaces. *Journal of neural engineering*, 15(5):056013, 2018.

Chenglin Li, A Mike Burton, Géza Gergely Ambrus, and Gyula Kovács. A neural measure of the degree of face familiarity. *cortex*, 155:1–12, 2022.

Ren Li, Jared S Johansen, Hamad Ahmed, Thomas V Ilyevsky, Ronnie B Wilbur, Hari M Bharadwaj, and Jeffrey Mark Siskind. The perils and pitfalls of block design for EEG classification experiments. *IEEE transactions on pattern analysis and machine intelligence*, 43(1):316–333, 2021.

Yitong Li, Kafui Dzirasa, Lawrence Carin, David E Carlson, et al. Targeting eeg/lfp synchrony with neural nets. *Advances in neural information processing systems*, 30, 2017.

Zongyi Li, Nikola Kovachki, Kamyar Azizzadenesheli, Burigede Liu, Kaushik Bhattacharya, Andrew Stuart, and Anima Anandkumar. Fourier neural operator for parametric partial differential equations. *arXiv preprint arXiv:2010.08895*, 2020.

Marc R Nuwer, Giancarlo Comi, Ronald Emerson, Anders Fuglsang-Frederiksen, and Peter Rappelsburger. Ifcn standards for digital recording of clinical eeg. *Electroencephalography & Clinical Neurophysiology*, 106(3):259–261, 1998.

Yu Ouyang, Yang Liu, Liang Shan, Zhe Jia, Dongguan Qian, Tao Zeng, and Hong Zeng. Daeegvit: A domain adaptive vision transformer framework for eeg cognitive state identification. *Biomedical Signal Processing and Control*, 100:107019, 2025.

Simone Palazzo, Concetto Spampinato, Isaak Kavasidis, Daniela Giordano, Joseph Schmidt, and Mubarak Shah. Decoding brain representations by multimodal learning of neural activity and visual features. *IEEE transactions on pattern analysis and machine intelligence*, 43(11):3833–3849, 2020.

Tsvetomila Popova and Holger Wiese. Developing familiarity during the first eight months of knowing a person: A longitudinal eeg study on face and identity learning. *Cortex*, 165:26–37, 2023a.

Tsvetomila Popova and Holger Wiese. How quickly do we learn new faces in everyday life? neurophysiological evidence for face identity learning after a brief real-life encounter. *Cortex*, 159: 205–216, 2023b.

Yonghao Song, Qingqing Zheng, Bingchuan Liu, and Xiaorong Gao. Eeg conformer: Convolutional transformer for eeg decoding and visualization. *IEEE transactions on neural systems and rehabilitation engineering: a publication of the IEEE Engineering in Medicine and Biology Society*, 31:710–719, 2023.

Yonghao Song, Bingchuan Liu, Xiang Li, Nanlin Shi, Yijun Wang, and Xiaorong Gao. Decoding natural images from eeg for object recognition. In *International conference on learning representations*, volume 2024, pp. 47648–47665, 2024.

Concetto Spampinato, Simone Palazzo, Isaak Kavasidis, Daniela Giordano, Nasim Souly, and Mubarak Shah. Deep learning human mind for automated visual classification. In *Proceedings of the IEEE conference on computer vision and pattern recognition (CVPR)*, pp. 6809–6817, 2017.

Mengdan Sun, Menglei Yao, and Xiaoqing Gao. How the percept of face familiarity unfolds over time. *Journal of Cognitive Neuroscience*, pp. 1–14, 2026.

Christian Szegedy, Wei Liu, Yangqing Jia, Pierre Sermanet, Scott Reed, Dragomir Anguelov, Dumitru Erhan, Vincent Vanhoucke, and Andrew Rabinovich. Going deeper with convolutions. In *Proceedings of the IEEE conference on computer vision and pattern recognition*, pp. 1–9, 2015.

Hind Taud and Jean-Franccois Mas. Multilayer perceptron (mlp). In *Geomatic approaches for modeling land change scenarios*, pp. 451–455. Springer, 2017.

Laurens Van der Maaten and Geoffrey Hinton. Visualizing data using t-sne. *Journal of machine learning research*, 9(11), 2008.

Holger Wiese, Simone C Tüttenberg, Brandon T Ingram, Chelsea YX Chan, Zehra Gurbuz, A Mike Burton, and Andrew W Young. A robust neural index of high face familiarity. *Psychological science*, 30(2):261–272, 2019.

Holger Wiese, Tsvetomila Popova, Linda H Lidborg, and A Mike Burton. The temporal dynamics of familiar face recognition: Event-related brain potentials reveal the efficient activation of facial identity representations. *International journal of psychophysiology*, 204:112423, 2024a.

Holger Wiese, Tsvetomila Popova, Maya Schipper, Deni Zakriev, A Mike Burton, and Andrew W Young. How neural representations of newly learnt faces change over time: Event-related brain potential evidence for overnight consolidation. *cortex*, 171:13–25, 2024b.

Sanghyun Woo, Jongchan Park, Joon-Young Lee, and In So Kweon. Cbam: Convolutional block attention module. In *European conference on computer vision*, pp. 3–19. Springer, 2018.

Xiaoqian Yan, Friederike GS Zimmermann, and Bruno Rossion. An implicit neural familiar face identity recognition response across widely variable natural views in the human brain. *Cognitive neuroscience*, 11(3):143–156, 2020.

Xiaoqian Yan, Angélique Volfart, and Bruno Rossion. A neural marker of the human face identity familiarity effect. *Scientific reports*, 13(1):16294, 2023.

Wuxia Zhang, Yang Xin, Shibo Lv, Xin Zhang, Xiang Zhong, and Jianmin Jiang. Eeg-face: A facial-image stimulated eeg data-set for analysis of brain perceived multimedia. In *Proceedings of the 33rd ACM International Conference on Multimedia*, pp. 12815–12821, 2025.

A Appendix

A.1 Sanity Check

For the 40-way face-identity decoding task, the theoretical Top-1 chance level is 2.50%. As a sanity check, we additionally estimate the empirical chance level by randomly shuffling the identity labels while keeping the remaining training and evaluation protocol unchanged, and the corresponding results are listed in Table 5. As seen, the resulting accuracy is 2.37%, closely matching the theoretical chance level. In contrast, EEG-STAFF achieves 7.81% Top-1 accuracy under the original identity labels, confirming that the observed decoding performance cannot be explained by chance-level classification.

Table 5: Sanity check for our investigations on facial identity decoding, where the experimental chance is obtained by randomly shuffling identity labels.

Condition	**Top-1 (%)**
Theoretical chance	2.50
Experimental chance	2.37
EEG-STAFF	7.81

A.2 Participant-level Temporal Statistical Analysis

To complement the participant-averaged temporal results reported in the main paper, we further assess the Pre-Fam–Post-Fam difference at the participant level for EEG-STAFF. For each temporal window, a two-sided paired t-test is conducted across the five participants and the results are summarized in Table 6. As seen, all temporal windows show significant Post-Fam improvements ($p < 0.001$). These participant-level results not only provide additional statistical support for the familiarity-associated decoding improvement, but also demonstrate that the 100–300 ms enhancement is not driven by a single participant.

Table 6: Participant-level statistical analysis of the temporal familiarity-associated improvement for EEG-STAFF.

Window	**Gain**	$t(4)$	p
0 – 100 ms	+0.52	14.22	< 0.001
100–200 ms	+1.29	9.20	< 0.001
200–300 ms	+1.48	10.19	< 0.001
300–400 ms	+1.06	12.25	< 0.001
400–500 ms	+0.67	14.65	< 0.001

A.3 Evaluation on Public EEG Benchmarks

We further evaluate the generalization of the proposed EEG-STAFF on two public EEG visual-decoding benchmarks, EEG-Face (Zhang et al., 2025) and THINGS-EEG (Gifford et al., 2022).

EEG-Face. EEG-Face is a facial-image-stimulated EEG dataset for 40-way single-trial face-identity decoding under randomized stimulus presentations. From the results given Table 7, it can be seen that EEG-STAFF achieves 3.8% Top-1 and 16.1% Top-5 accuracy, outperforming all the compared baselines.

THINGS-EEG. THINGS-EEG contains EEG responses elicited by diverse natural object concepts. Following the contrastive decoding framework of NICE-EEG (Song et al., 2024), we replace its EEG encoder with EEG-STAFF comparative evaluations and the results are listed in Table 7. As seen again, our proposed EEG-STAFF achieves the best average performance, with 14.3% Top-1 and 40.8% Top-5 accuracy across all the ten participants.

Table 7: Listing of identity decoding results on EEG-Face and THINGS-EEG.

Model	EEG-Face		THINGS-EEG	
	Top-1	Top-5	Top-1	Top-5
LSTM (Graves, 2012)	3.3	14.1	–	–
MLP (Taud & Mas, 2017)	3.1	13.5	–	–
CNN (Li et al., 2021)	3.4	14.4	–	–
EEGNet (Lawhern et al., 2018)	3.4	14.7	13.1	38.4
EEGChannelNet (Palazzo et al., 2020)	3.2	14.2	–	–
SyncNet (Li et al., 2017)	3.4	14.8	–	–
EEGConformer (Song et al., 2023)	3.3	14.1	11.1	33.8
NICE-EEG (Song et al., 2024)	3.2	14.1	13.8	39.5
DAEEGViT (Ouyang et al., 2025)	3.3	14.5	12.7	37.7
EEG-STAFF	**3.8**	**16.1**	**14.3**	**40.8**

A.4 Feature Geometry Metrics

In this section, we provide further supplementary details on the quantitative feature-geometry computation reported in Fig. 4. After L_2 normalization, the cosine distance between two feature representations is defined as

$$d(\mathbf{z}_i, \mathbf{z}_j) = 1 - \mathbf{z}_i^\top \mathbf{z}_j. \tag{6}$$

We then compute the average intra-identity and inter-identity distances as

$$D_{\text{intra}} = \mathbb{E}[d(\mathbf{z}_i, \mathbf{z}_j) \mid y_i = y_j,\ i \neq j]\,,$$
$$D_{\text{inter}} = \mathbb{E}[d(\mathbf{z}_i, \mathbf{z}_j) \mid y_i \neq y_j]\,. \tag{7}$$

A smaller D_{intra} indicates greater within-identity compactness, whereas a larger D_{inter} indicates stronger between-identity separation.

A.5 EEG Recording and Preprocessing

EEG signals are acquired using a 128-channel GREENTEK system arranged according to the international 10–10 system Nuwer et al. (1998) and amplified using a BrainVision actiCHamp Plus amplifier. The raw EEG signals are sampled at 5,000 Hz and subsequently downsampled to 1,000 Hz for analysis. In summary, our collection of EEGs can be highlighted as: (i) re-referencing to the linked earlobe electrodes A1/A2; (ii) zero-phase Butterworth band-pass filtering from 0.3 to 40 Hz together with a 50 Hz notch filter; (iii) ocular artifact removal using Independent Component Analysis (ICA); (iv) semi-automatic rejection of residual noise and recording artifacts; (v) epoch segmentation from -200 ms to $+500$ ms relative to stimulus onset; (vi) baseline correction using the -200 to 0 ms pre-stimulus interval; and (vii) multivariate noise normalization.

After baseline correction, only the 0–500 ms post-stimulus interval was retained for subsequent decoding. And after re-referencing, the two reference electrodes A1/A2 were excluded from the decoding input. Each EEG trial is therefore represented as a 126×500 spatiotemporal matrix, where 126 corresponds to the remaining EEG channels and 500 corresponds to the 500-ms post-stimulus response sampled at 1,000 Hz. The same preprocessing pipeline was applied to all participants, recording sessions, and stimulus conditions before subsequent decoding analysis.

A.6 Pre-experiment Familiarity Screening and Behavioral Validation

Before the EEG experiment, we conducted a pre-experiment familiarity screening to ensure that the selected identities were initially unfamiliar to the participants. Each participant viewed one representative frontal face image from each of the 40 identities and was asked whether they previously knew or recognized the person. All five participants reported no prior familiarity with any of the identities. The first EEG session (Pre-Fam) was conducted on the next day.

Before the second EEG session, participants completed the familiarization procedure described in the main paper. Familiarization performance was evaluated using the recognition task, and participants proceeded to the Post-Fam EEG session only after reaching the predefined criterion, which is 100% recognition accuracy with a mean response time below 5 s. All five participants reached this criterion before the Post-Fam EEG session. The final behavioral next summarized in Table 8.

Table 8: Response-time performance of all participants after reaching the familiarization criterion.

Participant	Max RT (s)	Mean RT (s)
S1	4.1	3.15
S2	3.6	2.78
S3	4.4	2.14
S4	3.5	2.56
S5	3.9	1.85

A.7 Occipito-temporal ROI Definition

Table 9: Electrodes included in the bilateral occipito-temporal ROI used for the ERP analysis in Fig. 3b.

Hemisphere	Electrodes
Left	TTP7h, TP7, TPP7h, P7, P9, PPO9h, PO7, PO9, POO9h, O1
Right	TTP8h, TP8, TPP8h, P8, P10, PPO10h, PO8, PO10, POO10h, O2

We provides supplementary details on the electrode selection and ERP computation used in Fig. 3b of the main paper. We focus on the bilateral occipito-temporal region, where face-sensitive ERP

responses such as the N170/N250 and familiarity-related activity are commonly observed (Sun et al., 2026; Li et al., 2022; Eick et al., 2021). The bilateral occipito-temporal ROI consists of 10 electrodes in each hemisphere, as listed in Table 9.

For each participant and condition, EEG trials were first averaged at each electrode to obtain electrode-wise ERP waveforms. The resulting waveforms were then averaged across the 20 selected electrodes to obtain a single bilateral occipito-temporal ERP waveform. The same procedure was applied independently to the Pre-Fam and Post-Fam conditions.